Available online at www.sciencedirect.com
ScienceDirect
Journal of Physics and Chemistry of Solids 68 (2007) 1003–1007
JOURNAL OF PHYSICS AND CHEMISTRY OF SOLIDS
www.elsevier.com/locate/jpcs

Low-temperature preparation and properties of ceramics with composition $(1-x)CaTiO_3-xPbF_2-xLiF$

L. Taïbi-Benziada*, H. Cherfouh

Faculty of Chemistry, USTHB, P.O. Box 32 El-Alia, 16311 Bab-Ezzouar, Algiers, Algeria

Abstract

Fluorinated ceramics with initial composition $(1-x)CaTiO_3+xPbF_2+xLiF$ were sintered at 950 °C. The X-ray diffraction (XRD) patterns of the samples showed the formation of a novel solid solution in the initial composition range $0\leqslant x\leqslant 0.125$. SEM observations were performed on fractured ceramics and DSC analyses were carried out from room temperature up to 600 °C. Three second-order phase transitions were detected for all the samples. Capacitors were prepared from the pre-sintered ceramics then dielectric measurements were performed as a function of temperature in the frequency range 10^2–4×10^7 Hz. The ε'_r-T curves exhibit the profile of dielectrics for class I capacitors, however the values of $\tan\delta$ are too high ($\tan\delta\geqslant 1\%$).

Keywords: D. Dielectric properties; D. Phase transitions

1. Introduction

The interest for ABO_3 materials is expanding very fast worldwide due to their large range of applications in several fields and especially in microelectronics. Among these applications one can cite as examples capacitors, sensors, resonators, piezoelectric actuators, pyroelectric infrared detectors, electro-optical modulators and computer memories [1–5]. Nowadays, $ATiO_3$ ceramics with perovskite structure like $BaTiO_3$ and $SrTiO_3$ became the heart of smart systems with high level of intelligence. In the race for manufacturing better computer memories, the solid solution between barium and strontium titanates $Ba_{1-x}Sr_xTiO_3$ (BST) is very attractive for the development of ferroelectric random access memories (FRAMs) which could achieve the gigabits density. In the future, dynamic random access memories (DRAMs) and hard disks (HDD) in computers will be replaced with FRAMs which are non-volatile memories [6–8].

The purpose of our work is first of all the search of new oxifluoride phases in the chemical system $CaTiO_3$–PbF_2–LiF, then the investigation of the properties in $(Ca,Pb)(Ti,Li)(O,F)_3$ ceramics sintered at low temperature.

The perovskite $CaTiO_3$ that is the host material in our study undergoes a sequence of phase transitions. At room temperature, this compound crystallizes in an orthorhombic lattice with *Pbnm* space group. Each unit cell of calcium titanate contains four formula units and the lattice parameters are: $a=5.385$ Å, $b=5.445$ Å, $c=7.646$ Å. With increasing temperature, $CaTiO_3$ transforms first from orthorhombic (*Pbnm*) to tetragonal (*I4/mcm*) at 1398 K then to cubic (*Pm3m*) at 1523 K [9]. During the last decade, the structure of $CaTiO_3$-based materials has been studied extensively as a function of temperature and pressure. Significant research effort was also directed towards synthetic routes to prepare calcium titanate and to optimize its properties owing to a wide range of applications for this perovskite. The most important property of $CaTiO_3$ is its ability to form a lot of solid solutions with lanthanides and actinides and therefore, calcium titanate could serve as host matrix for the immobilization of high-level radioactive wastes [10,11]. On the other hand, some non-stoichiometric $CaTiO_3$-based perovskites with formula $Ca_{1-x}Sr_xTi_{1-y}M_yO_{3-\delta}$ (M = Fe, Co, Cr or Ni) could be used as catalysts for partial oxidation of light hydrocarbons, thanks to their ability to supply directly oxygen

*Corresponding author. Fax: 213 21 24 73 11.
E-mail address: ikra@wissal.dz (L. Taïbi-Benziada).

0022-3697/$ - see front matter © 2007 Elsevier Ltd. All rights reserved.
doi:10.1016/j.jpcs.2007.01.005

from the oxides to surface-adsorbed species [12]. The substitution of Ti^{+IV} by Nb^{+V} induces a strong change in the electrical and optical properties of Ca(Ti,Nb)O_3 or CNTO phases that make them of interest in the fabrication of multilayer optical devices [13]. The addition of Ga to $CaTiO_3$:Pr perovskite enhances the luminescence intensity and the obtained compounds could find an application in field emission displays (FEDs) [14]. Moreover, $CaTiO_3$ has a large positive temperature coefficient of the resonant frequency τ_f and forms solid solutions with other compounds with negative τ_f yielding materials with an almost zero τ_f [15,16]. Therefore, $CaTiO_3$ is a promising material for communications equipment operating at microwave frequencies (UHF and SHF). The objective of our study is to prepare new dielectric ceramics related to $CaTiO_3$ at a temperature lower than 1000 °C, which could be used in the fabrication of future capacitors.

2. Experimental procedures

Commercial powders of $CaCO_3$, TiO_2 (rutile), PbF_2 and LiF were used in our study. All these starting materials were MERCK products of high-purity (99.99%) or superpure quality. Calcium carbonate and titanium oxide were dried up in an oven at 300 °C for 72 h to eliminate moisture. These powders were then weighed in stoichiometric composition (Ca/Ti = 1), mixed thoroughly and milled in an agate mortar. The obtained mixture was calcined at 850 °C for 8 h in a platinium capsule. After cooling, the powder was remilled and annealed at the same temperature for 2 h. The fluorides PbF_2 and LiF were dessicated under vacuum at 150 °C for 4 h to avoid their hydrolysis during the sintering. Ceramics with initial composition $(1-x)CaTiO_3 + xPbF_2 + xLiF$ were prepared using raw $CaTiO_3$ (distribution grain size 50–500 μm).

The appropriate amounts of calcium titanate, lead and lithium fluorides were homogenized in an agate mortar and dry ground for 30 min in a glove box. The powders thus obtained were compacted into tablets with a diameter of 13 mm under a pressure of 10^2 MPa. Finally, the pellets were placed on platinium plates and sintered by the conventional route at 950 °C for 4 h in an electrical furnace outside the box. The pellets were weighed before and after sintering.

The oxifluorides obtained were investigated by several methods: X-ray diffraction (XRD), scanning electron microscopy (SEM), differential scanning calorimetry (DSC) and dielectric measurements (DE). The XRD patterns were recorded at room temperature using a PHILIPS PW 1710 diffractometer with the Cu $K_{\alpha 1}$ monochromatic radiation ($\lambda = 1.5406$ Å) by step scanning of 0.02° in the 2θ range 5–80° and a counting time of 0.5 s per step. A PHILIPS LX 30 SEM operating at accelerating voltage of 20 kV and a magnification of 8000 times was used to probe the sample microstructure. Prior to SEM observations, the ceramics were fractured and then coated with a carbon (C) film in order to increase the sample conductivity. The DSC analyses were performed on heating under nitrogen gas between room temperature and 600 °C with a rate of 10 °C min^{-1} using a Perklin-Elmer machine. Two kinds of DE measurements were carried out under helium gas. In the first ones, the relative permittivities ε'_r (real part) and ε''_r (imaginary component) were measured on heating (25 °C $\leqslant T \leqslant$ 550 °C) at various frequencies (10^2, 5×10^2, 10^3, 5×10^3, 10^4, 5×10^4, 10^5, 2×10^5 Hz) by means of a Wayne-Kerr capacitance bridge. In the second ones, ε'_r and ε''_r were collected at room temperature as a function of frequency (10^5 Hz $\leqslant f \leqslant 4\times10^7$ Hz) using a Hewlett-Packard (HP 4194A) analyzer. Before each measurement, the circular faces of the ceramic were electroded by sputter deposition of gold (Au) to make a capacitor, then heated in the cell under vacuum at 150 °C for 2 h to prevent any contribution of water vapor in the dielectric characteristics.

3. Results and discussion

The loss in ceramic's weight is negligible and, therefore, we can deduce that the final and the initial compositions of the ceramics are close to one another. $CaTiO_3$ and (Ca,Pb)(Ti, Li)$(O,F)_3$ samples behave differently during the sintering process. Pure $CaTiO_3$ ceramics are very brittle even when sintered at 1200 °C. On the other hand, the fluorinated ceramics are very hard and the relative density reaches 95%. The relative shrinkages on ceramic diameter $\Delta\Phi/\Phi$ of the oxifluorides are in the range 14–17.5%, whereas the shrinkage of $CaTiO_3$ sample sintered at 950 °C is about 2% and does not exceed 5% after sintering at 1200 °C (Table 1). Larger is the amount of $PbF_2 + LiF$ additive and greater is the shrinkage. The greatest value of $\Delta\Phi/\Phi$ is obtained for $x = 12.5\%$.

Table 1
Shrinkage coefficients, lattice parameters and volume for ceramics with initial composition $(1-x)CaTiO_3 + xPbF_2 + xLiF$

X	$\Delta\Phi/\Phi$ (%)	a (Å)	b (Å)	c (Å)	V (Å^3)
0	1.9	5.443(7)	7.653(1)	5.376(8)	223.938
0.025	14	5.456(1)	7.651(1)	5.370(1)	224.164
0.05	14.6	5.446(8)	7.654(1)	6.379(8)	224.216
0.075	16.5	5.462(3)	7.653(5)	5.371(3)	224.511
0.10	16.8	5.454(7)	7.672(1)	5.373(7)	224.822
0.125	17.5	5.451(5)	7.672(6)	5.380(4)	224.991

As results of the XRD study, a solid solution was formed by the addition of PbF_2 and LiF to $CaTiO_3$. It occurs in the $0 \leqslant x \leqslant 0.125$ initial composition range. Beyond $x = 0.125$ the ceramics are polyphase. The room-temperature XRD spectra of both $CaTiO_3$ and the sample corresponding to $x = 0.05$ are reported in Fig. 1. As seen, these patterns are similar to each other and the isomorphism between the two samples is evident. The peaks were indexed in an orthorhombic symmetry and Table 1 gives the lattice parameters (a, b, c) and volume (V) of the oxifluorides. As we can take it from this table, the variation of V with increasing PbF_2 and LiF content is negligible and the orthorhombic perovskite structure of pure $CaTiO_3$ is not disturbed at all when calcium, titanium and oxygen ions are partially substituted by Pb^{2+}, Li^+ and F^-, respectively.

Concerning the SEM observations, the microstructural analyses confirmed the results obtained by the XRD study. The ceramics are single phases with a residual intergranular porosity varying between 5% and 8% as x decreases from 12.5% to 2.5%. Fig. 2 reports the scanning electron micrograph of the fracture for sample with initial composition $(1-x)CaTiO_3 + xPbF_2 + xLiF$. The micrograph is not smooth grained. The oxifluoride is composed of round and rectangular particles, which are clearly visible with a grain size of about 1–2 μm.

At this stage of investigation by taking into account the high values of shrinkages (Table 1), the low porosity and the XRD data, we can conclude that the additive $PbF_2 + LiF$ plays simultaneously a double role: as a substituent which enters the host lattice to form the $(Ca,Pb)(Ti,Li)(O,F)_3$ phases and as a sintering chemical agent to improve the compactness and the density of the ceramics.

The DSC analyses reveal three thermal phenomena for each sample. These transformations are accompanied by small changes in enthalpy and, therefore, we can conclude that the $CaTiO_3$ structure does not change so much. These phenomena are ascribed to second-order phase transitions with structural changes in space group without any disturbance in the orthorhombic lattice of $CaTiO_3$. Table 2 reports the values of the phase transition temperatures (T_1, T_2, T_3) and the heat capacities (C_{p1}, C_{p2}, C_{p3}) at, respectively, T_1, T_2 and T_3.

The dielectric measurements display the same profile for the temperature dependence of the dielectric permittivities ε'_r and ε''_r. The variation of ε'_r and ε''_r for a ceramic of $CaTiO_3$ sintered with the aid of 5 mol% of $PbF_2 + LiF$ is illustrated in Fig. 3 from room temperature up to 550 °C. In the temperature range 25–250 °C, ε'_r and ε''_r are frequency independent. The real component decreases progressively whereas the imaginary part of the permittivity is very stable with increasing temperature. Between 250 and 450 °C, the $\varepsilon'_r - T$ and $\varepsilon''_r - T$ curves exhibit a very broad peak. The maximum occurs around 400 °C and the values of ε'_r and ε''_r decrease as the frequency increases, wihout any displacement of the maximum toward high or low temperature. Beyond 450 °C, an increase of ε'_r and ε''_r with temperature is observed due especially to the contribution of the electrical conductivity of Li^+ ion on the dielectric characteristics.

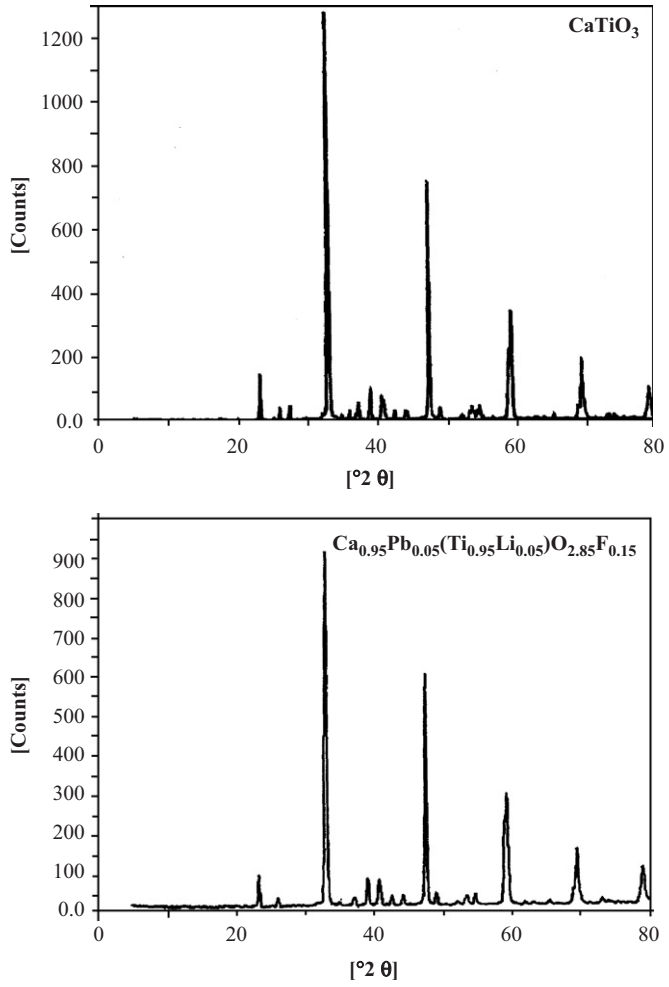

Fig. 1. XRD patterns of $CaTiO_3$ and $0.95CaTiO_3 + 0.05PbF_2 + 0.05LiF$ sample sintered at 950 °C.

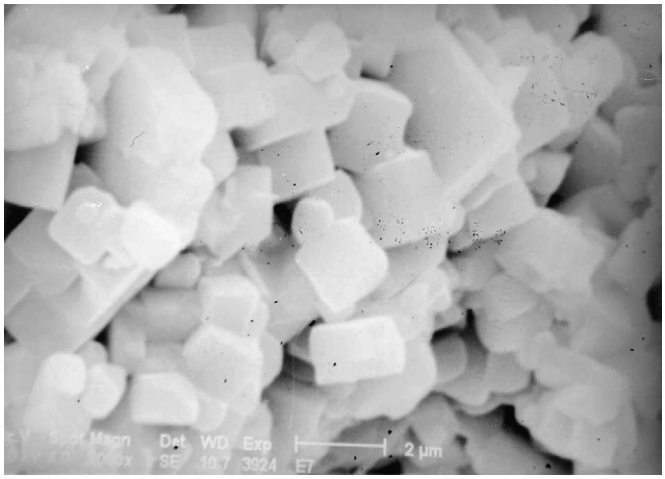

Fig. 2. Scanning electron micrograph of the fracture of $0.95CaTiO_3 + 0.05PbF_2 + 0.05LiF$ ceramic.

Table 2
Phase transition temperatures and heat capacities for $(1-x)CaTiO_3+xPbF_2+xLiF$ samples sintered at 950 °C

x	T_1 (K)	T_2 (K)	T_3 (K)	C_{p1} ($J\,mol^{-1}\,K^{-1}$)	C_{p2} ($J\,mol^{-1}\,K^{-1}$)	C_{p3} ($J\,mol^{-1}\,K^{-1}$)
0	—	—	—	—	—	—
0.025	702	748	805	8.2787	2.2338	4.1393
0.05	678	715	742	16.7230	22.2974	13.5317
0.075	605	705	748	2.2209	24.8398	39.4514
0.10	565	634	778	1.5846	7.0113	38.8688
0.125	512	630	813	7.9188	10.7470	11.5114

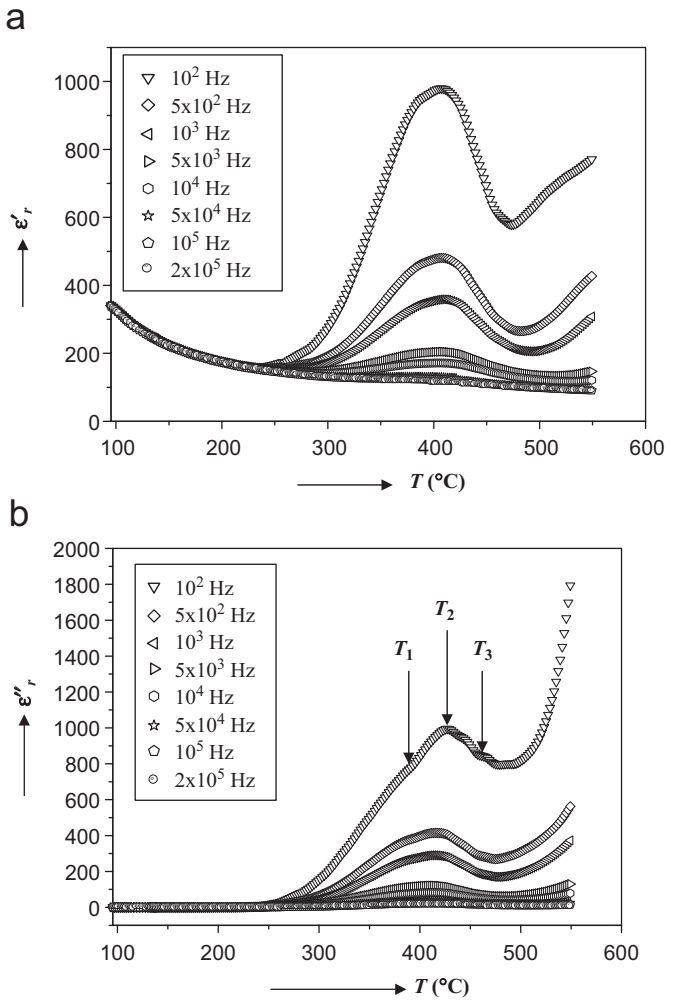

Fig. 3. Variation of permittivity as a function of temperature at various frequencies: (a) real component and (b) imaginary part for ceramic corresponding to $x = 0.05$.

The very wide peak is probably due to the overlap of the three thermal phenomena detected by DSC. The maximum could be attributed to the phase transition at T_2 while the phase transitions at T_1 and T_3 appear as inflection points, which are more visible on $\varepsilon''_r - T$ curve, before and after the maximum at T_2.

Fig. 4 depicts the $\varepsilon'_r - \log f$ and $\varepsilon''_r - \log f$ curves at room temperature for the sample corresponding to $x = 0.05$ and typical for all sintered ceramics. With the increase of

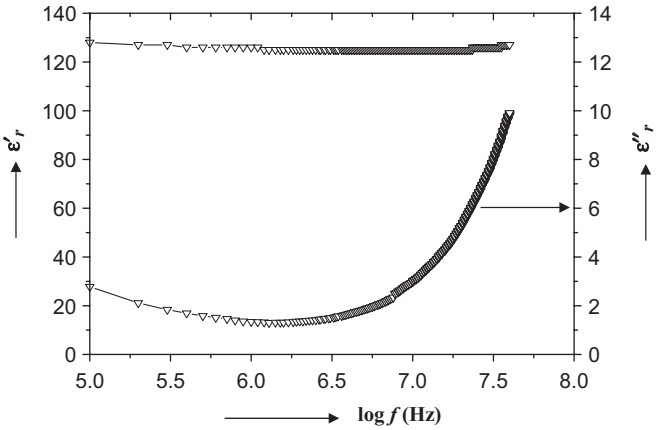

Fig. 4. Variation of the real and the imaginary permittivity as a function of frequency at room temperature of $0.95CaTiO_3+0.05PbF_2+0.05LiF$ ceramic.

frequency, the real permittivity is practically constant with a value of ~130 while the imaginary one decreases slightly from ~3 to ~1 in the frequency range $10^5-3\times10^6$ Hz then increases strongly beyond 3×10^6 Hz.

4. Conclusion

The fluoride mixture of PbF_2 and LiF is a suitable chemical agent to sinter $CaTiO_3$ at low temperature ($T_{sint.} = 950\,°C$), the relative density of the deriving ceramics reaches 95%. The addition of lead and lithium fluorides to calcium titanate allowed us to obtain new oxyfluorides $(Ca,Pb)(Ti,Li)(O,F)_3$. The triple substitution Ca–Pb, Ti–Li and O–F occurs in the $0\leqslant x\leqslant0.125$ initial composition range and induces no significant change in the $CaTiO_3$ cell which remains orthorhombic whatever the value of x is. Three second-order phase transitions are detected by DSC and confirmed by dielectric measurements. These materials could be of interest in several technological applications and particularly in the production of capacitors.

References

[1] J.C. Niepce, J.M. Haussonne, $BaTiO_3$: matériau de base pour les condensateurs céramiques, 1 and 2, Eds Septima, 1994.

[2] D.H. Yoon, B.I. Lee, Processing of barium titanate tapes with different binders for MLCC applications—Part II: comparison of the properties, J. Eur. Ceram. Soc. 24 (2004) 753–761.
[3] D. Zhou, Y. Chen, D. Zhang, H. Liu, Y. Hu, S. Gong, Fabrication and characterization of the multilayered PTCR ceramic thermistors by slip casting, Sensors Actuators A 116 (2004) 450–454.
[4] L. Taïbi-Benziada, A. Mezroua, R. Von Der Mûhll, $CaTiO_3$ related materials for resonators, Ceram. Silikaty 48 (4) (2004) 180–184.
[5] L. Taïbi-Benziada, Ferroelectric ceramics related to $BaTiO_3$ for Z5U multilayer capacitors, Mater. Sci. Forum 492–493 (2005) 109–114.
[6] F. Mücklich, H. Janocha, Smart materials—the "IQ" of materials in systems, Z. Metallkd. 87 (1996) 357–364.
[7] T. Shiosaki, The recent progress in the research and development for ferroelectric memory in Japan, in: Proceedings of COST 514 European Concerted Action Workshop on Ferroelectric Thin Films, 1997, pp. 19–44.
[8] J.F. Scott, New developments on FRAMS: [3D] structures and all-perovskite FETs, Mater. Sci. Eng. B 120 (1–3) (2005) 6–12.
[9] S.A.T. Redfern, High-temperature structural phase transitions in perovskite ($CaTiO_3$), J. Phys.: Condens. Matter 8 (1996) 8267–8275.
[10] Y. Hanajiri, H. Yokoi, T. Matsui, Y. Arita, T. Nagasaki, H. Shigematsu, Phase equilibria of $CaTiO_3$ doped with Ce, Nd and U, J. Nucl. Mater. 247 (1997) 285–288.
[11] Y.J. Shan, T. Nakamura, Y. Inaguma, M. Itoh, Preparation and dielectric characterizations of the novel perovskite-type oxides $(Ln_{1/2}Na_{1/2})TiO_3$ (Ln = Dy, Ho, Er, Tm, Yb, Lu), Solid State Ionics 108 (1998) 123–128.
[12] A.G. andersen, T. Hayakawa, T. Tsunoda, H. Orita, M. Shimizu, K. Takehira, Preparation and characterization of $CaTiO_3$-based perovskitic oxides as catalysts for partial oxidation of light hydrocarbons, Catal. Lett. 18 (1993) 37–48.
[13] R.P. Wang, C.J. Tao, Nb-doped $CaTiO_3$ transparent semiconductor thin films, J. Cryst. Growth 245 (2002) 63–66.
[14] S.Y. Kang, J.W. Byun, J.Y. Kim, K.S. Suh, S.G. Kang, Cathodo-luminescence enhancement of $CaTiO_3$:Pr^{3+} by Ga addition, Bull. Korean Chem. Soc. 24 (5) (2003) 566–568.
[15] J.S. Kim, C.I. Cheon, H.J. Kang, C.H. Lee, K.Y. Kim, S. Nam, J.D. Byun, Jpn. J. Appl. Phys. 38 (1999) 5633–5637.
[16] B. Jancar, D. Suvorov, M. Valant, Microwave dielectric properties and microstructural characteristics of aliovalently doped perovskite ceramics based on $CaTiO_3$, Key Eng. Mater. 206–213 (2002) 1289–1292.